The Astrophysical Journal, 612:L85–L88, 2004 September 1

THE USEFULNESS AND LIMITS OF CORONAGRAPHY IN THE PRESENCE OF PINNED SPECKLES

C. Aime
Laboratoire Universitaire d'Astrophysique de Nice, UMR 6525, Parc Valrose, 06108 Nice Cedex 2, France; claude.aime@unice.fr
and
R. Soummer[1]
Space Telescope Science Institute, 3700 San Martin Drive, Baltimore MD 21218; soummer@stsci.edu
Received 2004 April 9; accepted 2004 July 14; published 2004 July 27

ABSTRACT

In this Letter we study the utility and limitations of ground-based coronagraphy with adaptive optics (AO). In very high AO correction regimes, residual speckles are pinned on the diffraction rings of the Airy pattern. We show that this effect is due to small errors in the complex wave in the focal plane, amplified by the coherent part of the wave. The statistics of these speckles are fairly well described by a modified Rician distribution. The variance of the speckles, at high flux and at photon-counting levels, finds simple expressions. The total variance can be partitioned into two contributions: one that can be suppressed by a coronagraph and one that cannot. Different regimes can be identified. These results enable us to analyze when a coronagraph can defeat the noise variance, and they provide a criterion for the effectiveness of such instruments.

Subject headings: atmospheric effects — instrumentation: adaptive optics — techniques: high angular resolution

1. INTRODUCTION

Direct imaging of faint sources near a bright star (exoplanets, circumstellar disks) is a difficult task and is limited by many sources of noise, including the speckle noise. The problem is trying to detect a very faint object (a planet) above a bright background produced by the star diffraction wings. In the case of ground-based observations with adaptive optics (AO), the uncorrected aberrations of the wave front produce random intensity fluctuations of this background (residual speckles). Even at very high AO corrections, those speckles still exist but are "pinned" on the first diffraction rings for short-exposure images (Bloemhof et al. 2001; Sivaramakrishnan et al. 2002; Bloemhof 2003; Perrin et al. 2003). Several nulling or coronagraphic techniques have been proposed to cancel the starlight and achieve such a direct detection (e.g., Aime & Soummer 2003), and projects are under construction or study for ground- or space-based observations. We focus here on the effect of a coronagraph on the light fluctuations that limit the detection of faint sources. We limit the scope of this study to speckle noise and photon noise, and we leave for future study the other sources of noise (static or quasi-static aberrations, detector noise, etc.).

2. STATISTICAL MODEL FOR THE WAVE AMPLITUDE AND INTENSITY IN THE FOCAL PLANE WITHOUT CORONAGRAPH

Even for high-performance AO systems, the instantaneous point-spread function (PSF) is not a perfect Airy pattern, and speckles are pinned on the first rings as illustrated in Figure 1. These speckles produce a noisy background that limits the detection of faint sources. The goal of this study is to evaluate the impact of a coronagraph on the signal-to-noise ratio (S/N), analyzing the statistics of the intensity in the focal plane as a function of the radial position. We use a statistical model that was proposed by Goodman (1975) for the study of laser speckles and that was applied to AO images by Cagigal & Canales (1998, 2000) and Canales & Cagigal (1999a, 1999b, 2001) for the study of the statistics of AO images, as a function of the degree of correction. We start by describing the wave-front amplitude in the aperture plane and derive the statistics of the wave amplitude and of the intensity in the focal plane.

2.1. *Statistics of the Wave Amplitude in the Focal Plane*

In the general case, the wave-front amplitude at the entrance pupil can be written as the coherent sum of two terms, a deterministic term A corresponding to a perfect plane wave and a random term $a(x, y)$ corresponding to the uncorrected part of the wave front. This term can include either phase or amplitude errors:

$$\Psi_1(x, y) = [A + a(x, y)]P(x, y), \tag{1}$$

where the function $P(x, y)$ describes the aperture transmission. The complex amplitude of the wave in the focal plane is given by a scaled Fourier transform (FT) of this pupil amplitude (Goodman 1996):

$$\Psi_2(x, y) = \mathrm{FT}[\Psi_1(x, y)]_{x/(\lambda f), y/(\lambda f)} = \mathcal{F}[\Psi_1(x, y)], \tag{2}$$

where f denotes the telescope focal length, λ the monochromatic wavelength, and the symbol $\mathcal{F}$ the scaled FT; x and y are used as coordinates in both pupil and field. The focal complex amplitude is then

$$\begin{aligned}\Psi_2(x, y) &= A\mathcal{F}[P(x, y)] + \mathcal{F}[a(x, y)P(x, y)] \\ &= C(x, y) + S(x, y).\end{aligned} \tag{3}$$

The wave amplitude appears as a sum of a deterministic term C and a random term S, at each position in the focal plane. The term $C(x, y) = A\mathcal{F}[P(x, y)]$ is proportional to the wave amplitude without atmospheric turbulence (Airy pattern for a perfect telescope) and is a deterministic spatial function. The second component is a random term, associated with the speckles: $S(x, y) = \mathcal{F}[a(x, y)P(x, y)]$. This random term $S(x, y)$ is nonhomogeneous; its variance varies in the field.

[1] Michelson Fellow.

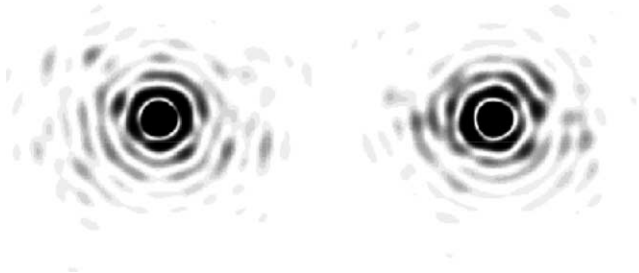

FIG. 1.—Illustration of two independent realizations of instantaneous AO PSFs. Pinned speckles on the diffraction rings are clearly visible. The simulated image has a Strehl ratio of 90% and was made with the PAOLA software package (Jolissaint 2004).

The statistics of the wave amplitude at each position in the focal plane can be easily derived from this model. The complex amplitude $S(x, y)$ is computed as a sum of phasors over the pupil aperture weighted by the random complex term $a(x, y)$. Assuming a large enough number of independent values of $a(x, y)$, i.e., a large number of coherent cells over the telescope aperture after AO correction, the complex amplitude $S(x, y)$ follows a circular Gaussian distribution whatever the statistics of $a(x, y)$, thanks to the central limit theorem. Therefore, the wave complex amplitude in the focal plane $\Psi_2(x, y)$ follows a circular Gaussian law, decentered by the mean of the amplitude $\langle \Psi_2(x, y) \rangle = C(x, y)$.

This problem is formally equivalent to the study of laser speckles over a coherent background in the context of holography. The statistics of $\Psi_2(x, y)$ were given by Goodman (1975):

$$\mathcal{P}(\xi, \eta) = \frac{1}{\pi \langle |S(x, y)|^2 \rangle} \exp\left\{ \frac{-[\xi - C(x, y)]^2 + \eta^2}{< |S(x, y)|^2 >} \right\}, \quad (4)$$

where ξ and η denote the real and imaginary part of $\Psi_2(x, y)$ at the position (x, y).

The deterministic term $C(x, y)$ can be taken as real without loss of generality. For example, in the case of a circular aperture of diameter D, we obtain the Airy amplitude $C(r) = D/[J_1(\pi D r)/(2r)]$, with $r = (x^2 + y^2)^{1/2}/(\lambda f)$. We give a numerical illustration of the statistics of $\Psi_2(x, y)$ in Figure 2 for two radial positions r.

2.2. *Statistics of the Light Intensity in the Focal Plane*

The instantaneous intensity in the focal plane is the modulus squared of the amplitude:

$$|\Psi_2(x, y)|^2 = |C(x, y)|^2 + |S(x, y)|^2 + 2 \text{ Re } [C^*(x, y) S(x, y)]. \quad (5)$$

The term coupling the deterministic and random parts (C and S) corresponds to the so-called speckle pinning, discussed by several authors, using a first-order phase expansion (Bloemhof et al. 2001; Bloemhof 2003, 2004) or higher order expansions (Sivaramakrishnan et al. 2002; Perrin et al. 2003).

The mean intensity (long-exposure image) is simply the sum of the deterministic diffraction pattern with a halo produced by the average of the speckles,

$$\langle |\Psi_2(x, y)|^2 \rangle = |C(x, y)|^2 + \langle |S(x, y)|^2 \rangle = I_c + I_s, \quad (6)$$

since $\langle S(x, y)^* \rangle = \langle S(x, y) \rangle^* = 0$ (circular Gaussian). We use the notations $I_c = |C(x, y)|^2$ for the intensity of the deterministic part of the wave, proportional to the perfect PSF, and $I_s = \langle |S(x, y)|^2 \rangle$ for the halo created by the speckle average. The model allows I_s to be a function that varies with the radial distance r, as is the case for an actual AO halo. AO PSF and halo structures have already been studied (Moffat 1969; Racine 1996; Racine et al. 1999).

At a given position in the focal plane, the pinned speckle term of equation (5) does not contribute to the mean intensity; it only contributes to the variance. This variance can be directly computed using the Gaussian property of $S(x, y)$. It is, however, interesting for a better understanding of the phenomenon to compute first the probability density function (PDF) of the intensity. In all cases, we emphasize that all these properties concern the speckle pattern at one point; it is unnecessary to invoke higher order spatial analysis for such a pointwise analysis. The PDF for the intensity, known as a *modified Rician density*, was given by Goodman (1975) and also used by Cagigal & Canales (1998, 2000, and reference therein):

$$\mathcal{P}_I(I) = \frac{1}{I_s} \exp\left(-\frac{I + I_c}{I_s} \right) I_0\left(\frac{2\sqrt{I}\sqrt{I_c}}{I_s} \right), \quad (7)$$

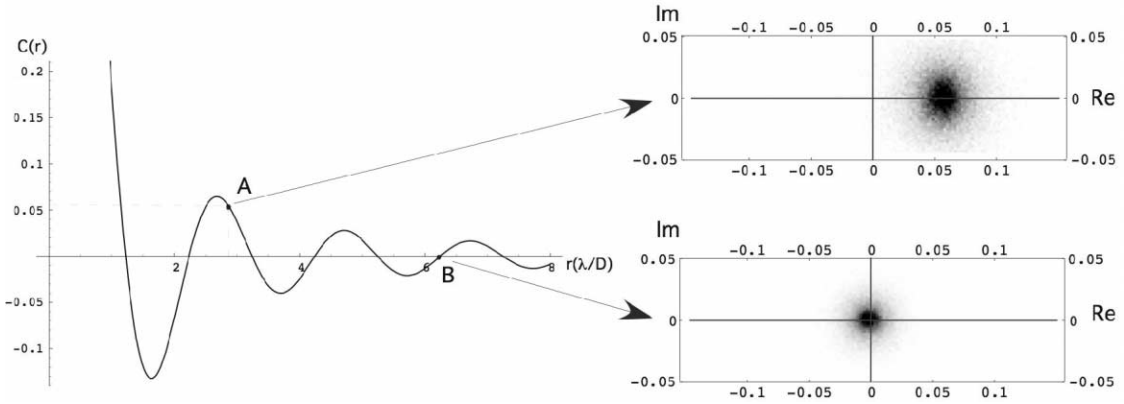

FIG. 2.—Illustration of the decentered Gaussian statistics of the wave amplitude $\langle \Psi_2(x, y) \rangle$, in the focal plane for two arbitrary spatial positions A and B. These figures have been obtained using 3000 independent AO-corrected phase screens provided by the PAOLA software. This illustration uses a perfect Airy pattern for the deterministic term $C(r)$. Note the decentered Gaussian statistics on the top of the diffraction ring. At the zeros of the term $C(r)$, the statistics become a centered circular Gaussian, similar to that of laser speckles without continuous background.

where I_0 denotes the zero-order modified Bessel function of the first kind. Examples of this Rician distribution are shown in Figure 3, for the same speckle intensity I_s and several levels of constant intensity I_c, corresponding to different positions in the field: at a given location in the focal plane, I_c will be proportional to the intensity of the perfect PSF (Airy pattern for a circular aperture). Depending on the amplitude of the Airy pattern at successive rings, the intensity I_c is alternatively large and small, and the variance of the speckles is amplified accordingly. At the zeros of the PSF, no amplification occurs, and the statistics are equivalent to that of a fully developed speckle pattern.

Speckle pinning can be easily explained from this result; speckle fluctuations are amplified by the coherent part of the wave that can be seen directly on the PDFs, where widths increase with I_c. Making $I_c = 0$ in equation (7) (at the zeros of the perfect PSF), the statistics reduces to the usual negative exponential density (Fig. 2) that corresponds to the same statistics as laser speckles. It is important to note that speckle fluctuations are not canceled but are just not amplified at the zeros of the perfect PSF (Fig. 1).

The planet adds a constant value m at its position (over a small region of the field). Using the approach developed by Aime (2000), the PDF is simply shifted of the quantity m, so that

$$P_{I,p}(I) = P_I(I - m). \tag{8}$$

This shift of the PDF does not change the variance.

3. VARIANCE OF THE INTENSITY

The variance of the intensity at and around the planet location in the image can be used as a simple criterion to evaluate the efficiency of a coronagraph. From the statistics of the residual speckles (eq. [7]), the variance finds a simple expression:

$$\sigma_I^2 = I_s^2 + 2I_sI_c. \tag{9}$$

This result was obtained by Goodman (1975) for the addition of a laser speckle pattern with a continuous background, and it was used by Cagigal & Canales (1998, 2000, and references herein) for the study of corrected PSF intensity statistics as a function of the degree of correction. Several routes to this result exist but are not discussed here. More details are given by Aime & Soummer (2004).

At low light levels, we must take into account the variance associated with photodetection (Poisson process), so the total variance is

$$\sigma^2 = \sigma_I^2 + \sigma_P^2, \tag{10}$$

where σ_P^2 is the variance associated with the Poisson statistics. In our notation, $\sigma_P^2 = I_c + I_s$ (the variance is equal to the mean for a Poisson process). The total variance is then

$$\sigma^2 = I_s^2 + 2I_sI_c + I_c + I_s. \tag{11}$$

A planet simply adds its variance m to the total variance, but this effect will be negligible for very faint sources. For brighter sources, compared to the level I_c, this term can be added easily.

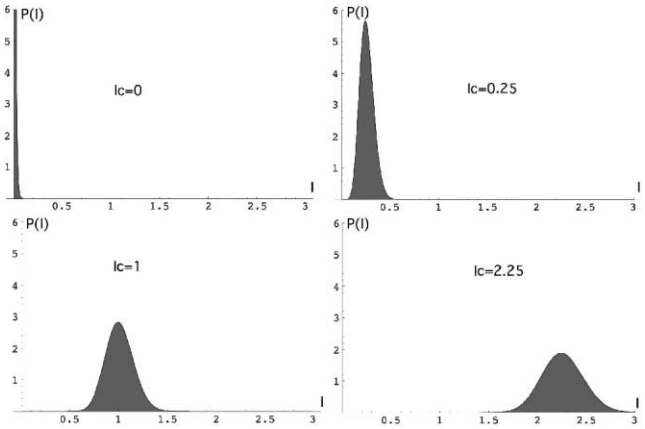

FIG. 3.—PDF of the light intensity at four different constant background intensity levels I_c and a single value of $I_s = 0.1$. High values of I_c correspond to locations near the perfect PSF maxima (rings), and low values of I_c correspond to locations near the zeros of the perfect PSF or far from the core. For $I_c = 0$ we have the pure speckle exponential statistics. The width of the distribution increases with an increase in the level of I_c. This explains speckle pinning; speckle fluctuations are amplified by the coherent addition of the perfect part of the wave.

4. THE UTILITY OF CORONAGRAPHY IN THE PRESENCE OF RESIDUAL AO SPECKLES.

Our goals are to determine under what conditions the use of a coronagraph will substantially reduce the speckle variance and to evaluate the efficiency of such a device. We consider the use of a perfect coronagraph that can remove the coherent part of the wave $C(x, y)$. The coronagraph will be ineffective at removing the speckle part $S(x, y)$. We first describe in this section what gain in S/N can be expected with a perfect system, and then we discuss the optimal coronagraphic rejection for a given AO correction and a real coronagraph.

The relevant information to analyze is how a coronagraph can defeat the noise variance. For that, we can partition the total variance of equation (11) into two contributions, σ_c^2 and σ_s^2. The first part σ_c^2 contains terms that can be affected by a coronagraph; they are the terms related to the perfect part of the wave, i.e., corresponding to the term I_c. The second part σ_s^2 contains the terms coming from the speckle term I_s only,

$$\sigma^2 = (2I_sI_c + I_c) + (I_s^2 + I_s) = \sigma_c^2 + \sigma_s^2, \tag{12}$$

with $\sigma_c^2 = 2I_sI_c + I_c$ and $\sigma_s^2 = I_s^2 + I_s$. Since a coronagraph can only affect the coherent part $C(x, y)$ of the wave, it can only have an effect on the variance σ_c^2, reducing (or canceling) the term I_c. The variance σ_s^2 will remain since the coronagraph will have no effect on I_s.

We can identify different regimes from equation (12), comparing the values of I_s and I_c. If $I_c \ll I_s$, which happens either far from the optical axis or with a perfect coronagraph, the variance reduces to $\sigma_s^2 = I_s^2 + I_s$. The level of intensity I_s equal to 1 photon pixel^{-1} is a limit of the regime between speckle and photon noise (the variance is dominated either by the speckle noise or by the photon noise).

If $I_c \gg I_s$, close to the optical axis (on the first few diffraction rings) or without a coronagraph, the variance becomes $\sigma_c^2 = 2I_cI_s + I_c$. One photon per pixel is also a limit of the regime. The transition domain for $I_c = I_s$ leads to the variance $\sigma_I^2 = 3I_s^2 + 2I_s$.

More generally, the study of the AO images without a co-

ronagraph can provide information on the efficiency of a coronagraph. A real coronagraph will be efficient in the part of the focal field where $\sigma_c^2 > \sigma_s^2$; it will reduce the contribution σ_c^2, and the ultimate performance will then be the speckle variance σ_s^2. From $\sigma_c^2 > \sigma_s^2$ we can deduce the following criterion for the efficiency of a coronagraph:

$$I_c > \frac{I_s(I_s + 1)}{2I_s + 1}. \quad (13)$$

At high flux, $I_s \gg 1$, and the condition of equation (13) is equivalent to $I_c^{(1)} > I_s/2$. At photon-counting rates $I_s \ll 1$, this limit is equivalent to $I_c^{(2)} > I_s$. In both cases, the order of magnitude is similar and does not depend on the number of photons. We can conclude that for either low or high flux, a coronagraph is efficient in terms of the S/N, as long as $I_c > I_s$ in the original AO images without a coronagraph.

To conclude, the main result is that a coronagraph for a given telescope and AO should reduce the contribution σ_c^2 lower than σ_s^2 everywhere in the field. It is therefore not necessary to build a coronagraph to reduce levels of continuous intensity I_c lower than the speckle level I_s.

The model used is very simple and can be improved, but our general conclusion is unlikely to change. Several other noise terms involved in the problem of high dynamic range imaging have not been taken into account in this study, e.g., detector or background noise. Static or quasi-static speckles from the optics are also an important issue and are not included in this model.

We give an example in Figure 4 to illustrate our conclusion, in which a coronagraph could reduce the variance by an order of magnitude on the first ring and be efficient out to the sevebth or eightth ring. These numbers are given here for illustration only and strongly depend on the actual AO characteristics and performance. The lower the halo I_s and the term σ_s^2, the greater the coronagraphic efficiency. This result can help the design of dedicated AO for coronagraphy; the levels and profiles of I_s and I_c directly impact the dynamic range and depend on the AO characteristics.

This study confirms that a coronagraph is a key element in a high dynamic range imaging instrument. It will tackle noise amplification from the continuous background, at high AO performance. Additional speckle reduction techniques are also necessary to defeat the residual noise.

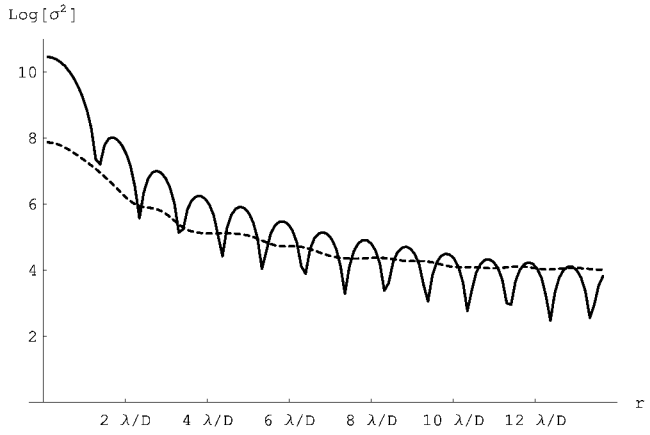

FIG. 4.—Illustration of σ_c^2 and σ_s^2, as a function of the radial position in the focal plane, without a coronagraph. The simulation is made for a 3.6 m telescope in the *H* band with a Strehl ratio of 90%, corresponding to the Lyot Project coronagraph on the AEOS telescope in Hawaii (Oppenheimer et al. 2003, 2004). A coronagraph will be efficient everywhere the variance σ_c^2 (*solid line*) is greater than σ_s^2 (*dashed line*). This simulation corresponds to a high-flux regime and is independent of the exposure time. PAOLA software (Jolissaint 2004) was used to simulate the AO.

The authors would like to thank Laurent Jolissaint for the PAOLA software and Anand Sivaramakrishnan and Russel Makidon for comments on the manuscript. Thanks are also due to the anonymous referee for interesting remarks. Rémi Soummer is supported by a Michelson Postdoctoral Fellowship, under contract with the Jet Propulsion Laboratory (JPL) funded by NASA. JPL is managed for NASA by the California Institute of Technology. This work is based on work partially supported by the National Science Foundation under grant AST-0215793 and has also been partially supported by the National Science Foundation Science and Technology Center for Adaptive Optics, managed by the University of California at Santa Cruz under cooperative agreement AST-9876783.

REFERENCES

Aime, C. 2000, J. Opt. A: Pure Appl. Opt., 2, 411
Aime, C., & Soummer, R., eds. 2003, Astronomy with High Contrast Imaging (EAS Publ. Ser. 8; Les Ulis: EDP Sciences)
———. 2004, in EUSIPCO 2004, 12th European Signal Processing Conf., 2004 September 6–10, Vienna, Austria, in press
Bloemhof, E. E. 2003, ApJ, 582, L59
———. 2004, Opt. Lett., 29, 159
Bloemhof, E. E., Dekany, R. G., Troy, M., & Oppenheimer, B. R. 2001, ApJ, 558, L71
Cagigal, M. P., & Canales, V. F. 1998, Opt. Lett., 23, 1072
———. 2000, J. Opt. Soc. Am. A, 17, 1312
Canales, V. F., & Cagigal, M. P. 1999a, J. Opt. Soc. Am. A, 16, 2550
———. 1999b, Appl. Opt., 38, 766
———. 2001, Opt. Lett., 26, 737
Goodman, J. W. 1975, in Laser Speckle and Related Phenomena, ed. J. C. Dainty (Berlin: Springer), 9
Goodman, J. W. 1996, Introduction to Fourier Optics (2nd ed.; New York: MacGraw-Hill)
Jolissaint, L. 2004, PAOLA Simulation Software (http://cfao.ucolick.org/software/paola.php)
Moffat, A. F. J. 1969, A&A, 3, 455
Oppenheimer, B. R., et al. 2004, Proc. SPIE, 5490, in press
Oppenheimer, B. R., Sivaramakrishnan, A., & Makidon, R. B. 2003, in The Future of Small Telescopes in the New Millennium, Vol. 3: Science in the Shadow of Giants, ed. T. D. Oswalt (ASSL Vol. 289; Dordrecht: Kluwer), 155
Perrin, M. D., Sivaramakrishnan, A., Makidon, R. B., Oppenheimer, B. R., & Graham, J. R. 2003, ApJ, 596, 702
Racine, R. 1996, PASP, 108, 699
Racine, R., Walker, G. A. H., Nadeau, D., Doyon, R., & Marois, C. 1999, PASP, 111, 587
Sivaramakrishnan, A., Lloyd, J. P., Hodge, P. E., & Macintosh, B. A. 2002, ApJ, 581, L59